

Material and methods

Accelerator

Our AB-BNCT system consists of a cyclotron accelerator that produces a proton beam of ~ 2 mA at 30 MeV, beam transport system, beam scanning system on the beryllium target, target cooling system, neutron-beam-shaping assembly (BSA), multileaf collimator, and an irradiation bed for patients in both sitting and decubitus positions. Fig. 1 shows a schematic layout of the BSA for production of epi-thermal neutrons.

The ${}^6\text{Li}(p,n)$ reaction at low proton energy is widely accepted as the most promising for epi-thermal neutron generation [9]. However, we selected the ${}^9\text{Be}(p,n)$ reaction with 30 MeV for our AB-BNCT system because: (1) the system using ${}^6\text{Li}(p,n)$ reaction needs an accelerator with a current of >5 mA to yield an intensity of epi-thermal neutron flux of $\lambda \times 10^9$ n/cm²/s. No accelerator is presently available to achieve such a high current; (2) it is difficult to stably operate a lithium target with heat >10 kW because the 180°C melting point of lithium is much lower than that of beryllium, which is 1278°C ; and (3) the ${}^9\text{Be}(p,n)$ reaction with 30 MeV has a higher neutron yield compared with the ${}^6\text{Li}(p,n)$ reaction. The neutron yield of the ${}^6\text{Li}(p,n)$ reaction with 1.9 MeV (near threshold) is about 2.4×10^{-6} (neutrons/proton) [9]. Whereas, the neutron yield of the ${}^9\text{Be}(p,n)$ reaction with 30 MeV is about 3.0×10^{-2} (neutrons/proton) [10].

The reaction of a proton with the beryllium target emits high energy neutrons at up to 28 MeV in the 0° direction. The 0° neutron yield is the largest. The BSA consists of lead, iron, calcium fluoride, and aluminum for reducing neutron energy and shaping an epi-thermal neutron beam. The BSA is surrounded by polyethylene material for shielding fast neutrons and for decreasing radiation to the patient's body. The γ -ray dose contamination in the treatment neutron beam increases because of γ -rays coming from the neutron capture in hydrogen materials such as polyethylene. How-

ever, the γ -ray dose contamination per epi-thermal neutron in a treatment beam under free-air conditions is 2.75×10^{-14} Gy cm² (epi-thermal region is from 0.5 eV to 40 keV). This value is sufficiently below than the IAEA-TECDOC-1223 target value of 2×10^{-13} [11].

KUR

KUR is a light water-moderated, tank-type nuclear research reactor, with a nominal power of 5 MW. The Heavy Water Neutron Irradiation Facility (HWNIF) is a bio-medical facility at KUR-RI. The facility has been previously described in detail [12,13]. The higher energy neutrons are moderated by the epi-thermal neutron moderator, which is the mixture of aluminum and heavy water (80%/20% in volume). The heavy-water spectrum shifter is installed outside of the epi-thermal neutron moderator, for control of the neutron-energy spectrum. The total heavy-water thickness can be changed from 0 to 90 cm in 10-cm increments. The thermal neutron filters of cadmium and boron are installed outside of the spectrum shifter, to regulate the thermal neutron component. The apertures of these filters are changed from 0 to 62 cm. Outside of the filters, the bismuth layer is placed for γ -ray elimination. In this facility, neutron beams with various energy spectra from almost pure thermal to epi-thermal are available by controlling the heavy-water thickness in the spectrum shifter, and by the opening and closing of the cadmium and boron thermal neutron filters.

Comparison of neutron spectra

A comparison has been carried out between the neutron spectra at the output port in air for AB-BNCT and RB-BNCT. For the KUR, the neutron spectrum was measured by activation of gold foils. For the accelerator-based neutron source, the neutron spectrum was obtained by simulations from a calculated neutron source.

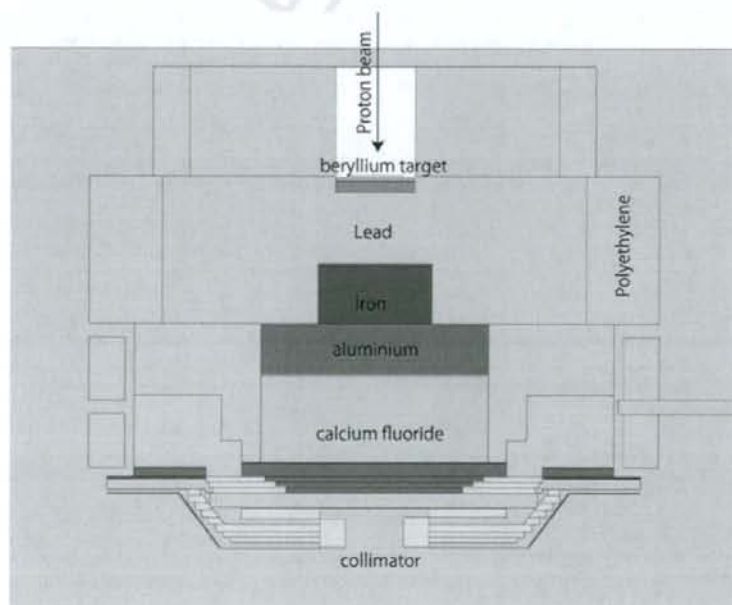


Fig. 1. Schematic layout of BSA for production of epi-thermal neutrons based on beryllium (p,n) reaction using 30 MeV proton beam.

Assumption and parameters for BNCT treatment planning

The conditions and parameters in BNCT treatment planning are summarized in Table 1. The parameters were approximately the same as those in our previous treatment planning studies on BNCT for multiple liver tumors and MPM [5,6]. The details for determination of each parameter have been described in our previous reports [5,6]. The compound biologic effectiveness (CBE) factors of the boron compounds in Table 1 were requested to convert the physical dose of BNCT to the photon-equivalent dose (Gy-Eq) and the relative biologic effectiveness (RBE) of each component of the beam. The CBE factors were used as an alternative RBE in evaluating the biologically equivalent absorbed dose by BNCT. This was because the same or different boron compounds might yield variable effects on different tissues, as a result of variations in the microdistribution of the boron compounds and the morphological character of the target cells. The CBE factors and RBE values for the tumors were the same as those used in clinical BNCT trials [14,15]. The CBE factors and RBE values for liver and lung were determined by experimental studies using rodents [16,17]. We adopted the value of 3.0 as the RBE value of ^{14}N (n,p) ^{14}C radiations and fast neutrons for liver. The value was greater than the RBE of fast neutron for hepatocytes reported by Ono et al. [18]. Use of the greater RBE for normal liver is expected to decrease the occurrence of radiation-induced liver disease in clinical situation.

The difference in the method between BNCT for multiple liver tumors and MPM was the drug delivery system (DDS) for the boron compounds. In BNCT for multiple liver tumors, borocaptate sodium (BSH), which has been employed as a boron compound in clinical BNCT trials for malignant glioma, was administered via the hepatic artery with vessel occlusion materials (lipiodol), according to our previous reports [3,5,7]. This DDS method is possible to deliver ^{10}B to liver tumors highly selectively [3]. In the present study, ^{10}B tumor/liver concentration ratio was assumed to be 20 according to our present study (Table 1) [3]. In BNCT for MPM, boronophenylalanine (BPA), another boron compound available in clinical trials, was administered intravenously [8]. In the MPM cases, ^{10}B tumor/liver or liver concentration ratio was assumed to be 3.5 (Table 1).

In BNCT for multiple liver tumors, the whole liver was defined as the clinical target volume (CTV). Three-port irradiation by anterior, right and posterior (ARP) beams was planned to deliver thermal neutrons to whole liver as homogeneously as possible [5]. Because the CTV for MPM was defined as the hemithorax, including the tumor and ipsilateral normal lung, the CTV was divided into upper and lower portions because of the limit in circular collimator size (maximum 25 cm). Each CTV was irradiated with anterior-

posterior (AP) beams or 20–30° anterior-oblique and posterior-oblique beams. The oblique beams were used to deliver greater doses to the tumors at mediastinal side compared to AP beams in some cases. Four-port irradiation was needed for covering the whole CTV.

Overview of BNCT treatment planning using the simulation environment for radiotherapy applications (SERA) system

Computed tomography (CT) images of four patients with multiple liver tumors and six with MPM were used in the present study. Three patients had right MPM, and the other three had left MPM. In four BNCT treatment plans for multiple liver tumors, a total of 11 liver tumors were evaluated.

We have already reported the treatment planning studies on BNCT for multiple liver tumors and MPM using KUR epi-thermal neutron beam data and the SERA system, a currently available BNCT treatment planning system. Details of the procedures in treatment planning using the SERA system have been described in our previous reports [5,6].

Dose-volume histogram (DVH) analysis

The SERA system can provide DVH data for each tumor or for the normal tissues as a whole. The maximum, minimum and mean doses to the tumors and normal tissues were assessed for each case. In radiotherapy for liver tumors and MPM, radiation-induced liver injury and radiation pneumonitis are dose-limiting toxicities, therefore, we set the doses delivered to normal liver and lung tissues as constraint doses. In the present study, 5.0 Gy-Eq of the mean liver and lung doses were set as the constraint doses. Under these conditions, each DVH parameter and irradiation time was compared between AB-BNCT and RB-BNCT. The doses delivered to the tumors with AB-BNCT and RB-BNCT were compared by means of Wilcoxon's signed-rank test.

Results

Neutron spectra comparison

Fig. 2 shows the neutron spectra at the output port produced by the accelerator-based neutron beam (1 mA, 30 MeV proton beam with the beryllium target) and epi-thermal neutron beam of HWNI in the KUR. The neutron beam produced by the accelerator was harder compared with that of the KUR. In comparison of the maximum numbers yielded per lethargy, the accelerator source produced neutrons approximately four orders of magnitude higher than KUR.

Comparison of dose distributions in BNCT for multiple liver tumors

Table 2 summarizes the DVH parameters for tumor and normal liver and irradiation time for three-port irradiation in AB-BNCT and RB-BNCT for multiple liver tumors. To compare irradiation time and dose distribution in tumors between AB-BNCT and RB-BNCT, all treatment plans were normalized to deliver mean doses of 5 Gy-Eq to the whole liver. The average irradiation time was 43.8 and 198.3 min in AB-BNCT and RB-BNCT, respectively. The averages of the maximum, mean and minimum doses delivered to all 11 tumors in the AB-BNCT were significantly higher than those in RB-BNCT (78.7 vs. 77.4 Gy-Eq, 68.1 vs. 65.1 Gy-Eq and 57.7 vs. 53.7 Gy-Eq, $p = 0.0023$, $p = 0.0040$, and $p = 0.0022$, respectively).

Fig. 3A shows the isodose distributions in the representative case with deep-seated liver tumor provided by RB-BNCT and AB-BNCT. AB-BNCT delivered higher dose to the tumor than RB-BNCT. Fig. 3B shows the depth-dose distribution profiles along the right

Table 1

^{10}B concentrations and RBE and CBE factors used for conversion of physical dose (Gy) to photon-equivalent dose (Gy-Eq).

	Liver tumor MPM	Liver	Lung
^{10}B concentration (ppm)	200.0	84.0	10.0
			(Liver tumor cases)
			24.0 (MPM cases)
RBE, CBE			
^{10}B (n, α) ^7Li	2.5	3.8 (CBE _{for BPA})	0.94 (CBE _{for BSH}) [*]
	(CBE _{for BSH})	4.25 (CBE _{for BPA}) [*]	2.3 (CBE _{for BPA}) [*]
^{14}N (n, p) ^{14}C	3.0	3.0	3.0
Fast neutron	3.0	3.0	3.0
γ -Ray	1.0	1.0	1.0

Abbreviations: RBE = relative biological effectiveness; CBE = compound biological effectiveness; MPM = malignant pleural mesothelioma; BSH = borocaptate sodium; BPA = boronophenylalanine.

^{*} Data from Suzuki et al. [16].

[†] Data from Kiger et al. [17].

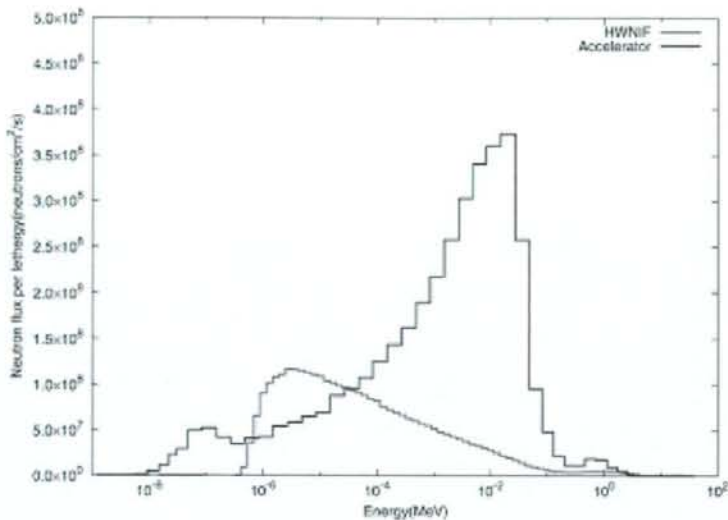


Fig. 2. Comparison of neutron spectrum between HWNIF and accelerator-based neutron source shaped with the BSA.

neutron beam axis which passed into the deep-seated liver tumor. The depth-dose profiles in the tumor located at a depth of 9.0–12.5 cm demonstrated that AB-BNCT delivered a higher dose than RB-BNCT. Fig. 3C shows the depth-ratio of thermal neutron fluence-rate (AB-BNCT to RB-BNCT) profiles along the same beam axis as in Fig. 3B. The ratio of thermal neutron fluence-rate increased from 3.9 to 6.3 at a depth of 1–12 cm, which was caused by the property of the accelerator-based neutron source which has a peak at higher energy in its neutron spectrum compared with that of the KUR as shown in Fig. 2.

Comparison of treatment parameters in BNCT for MPM

Table 3 compares the DVH parameters for tumor and normal lung and irradiation time for four-port irradiation in AB-BNCT and RB-BNCT for MPM. To compare irradiation time and dose distribution in the tumor between AB-BNCT and RB-BNCT, all treatment plans were normalized to deliver mean doses of 5 Gy-Eq to the whole of the ipsilateral lung. The average irradiation time in AB-BNCT and RB-BNCT were 29.9 and 134.7 min, respectively. The mean doses delivered to the MPM tumors by AB-BNCT and RB-BNCT were 20.2 and 19.9 Gy-Eq, respectively. The average of the maximum doses delivered to the MPM tumors by AB-BNCT was significantly lower than those with RB-BNCT (36.4 vs. 40.0 Gy-Eq, $p = 0.0253$). On the other hand, the average of the minimum doses delivered to the MPM tumors by AB-BNCT was significantly higher than those with RB-BNCT (4.6 vs. 4.3 Gy-Eq, $p = 0.0275$).

Table 2

Irradiation time and DVH parameters showing averages (with range) for liver tumors and normal liver.

Neutron source	Irradiation time (min)	Tumor			Liver		
		D_{max} (Gy-eq)	D_{mean} (Gy-eq)	D_{min} (Gy-eq)	D_{max} (Gy-eq)	D_{mean} (Gy-eq)	D_{min} (Gy-eq)
KUR	198.3 (177.0–216.8)	77.4 (49.3–104.6)	65.1 (33.8–84.2)	53.7 (20.7–76.5)	6.9 (6.4–7.4)	5.0*	1.9 (1.3–2.1)
Accelerator	43.8 (39.0–47.8)	78.7 (52.6–102.0)	68.1 (37.7–87.1)	57.7 (23.6–76.7)	6.7 (6.3–7.2)	5.0*	1.7 (1.1–2.2)

Abbreviations: DVH = dose-volume histogram; KUR = Kyoto University Research Reactor.

* The mean dose to the liver normalized to 5.0 Gy-Eq.

Fig. 4A shows the isodose distributions for the tumor in the representative case with MPM provided by RB-BNCT and AB-BNCT. AB-BNCT delivered higher dose to the MPM tumor located in the middle of the thorax compared to RB-BNCT. Fig. 4B shows the depth-dose distribution profiles along the anterior-posterior thermal neutron beam axis in the case of MPM. The tumor located at a depth of 9.0–12.5 cm received a greater dose with AB-BNCT compared with RB-BNCT. On the other hand, RB-BNCT delivered a greater dose to the tumor located at a depth of 3.5–5.0 cm. Fig. 4C shows the depth-thermal neutron flux ratio (AB-BNCT to RB-BNCT) profiles along the same beam axis as Fig. 4B. The thermal neutron flux ratio increased from 4.0 to 5.8 within a depth of 1–12 cm.

Discussion

In BNCT for multiple liver tumors and MPM, the most important feature of the AB-BNCT system under construction at our institute is capability to deliver three- or four-port irradiation within a reasonable treatment time (<1 h), including the time required for changing patient position. Shortening of irradiation time makes it possible to finish irradiation while maintaining a high ^{10}B concentration in the tumor, and to reduce the non-selective background dose. In addition, shortening of irradiation time provides comfort to the patients during irradiation and single or two-fractionated BNCT has economic benefits.

Another important feature of the AB-BNCT system is its capability of delivering greater doses to deep-seated tumors than RB-

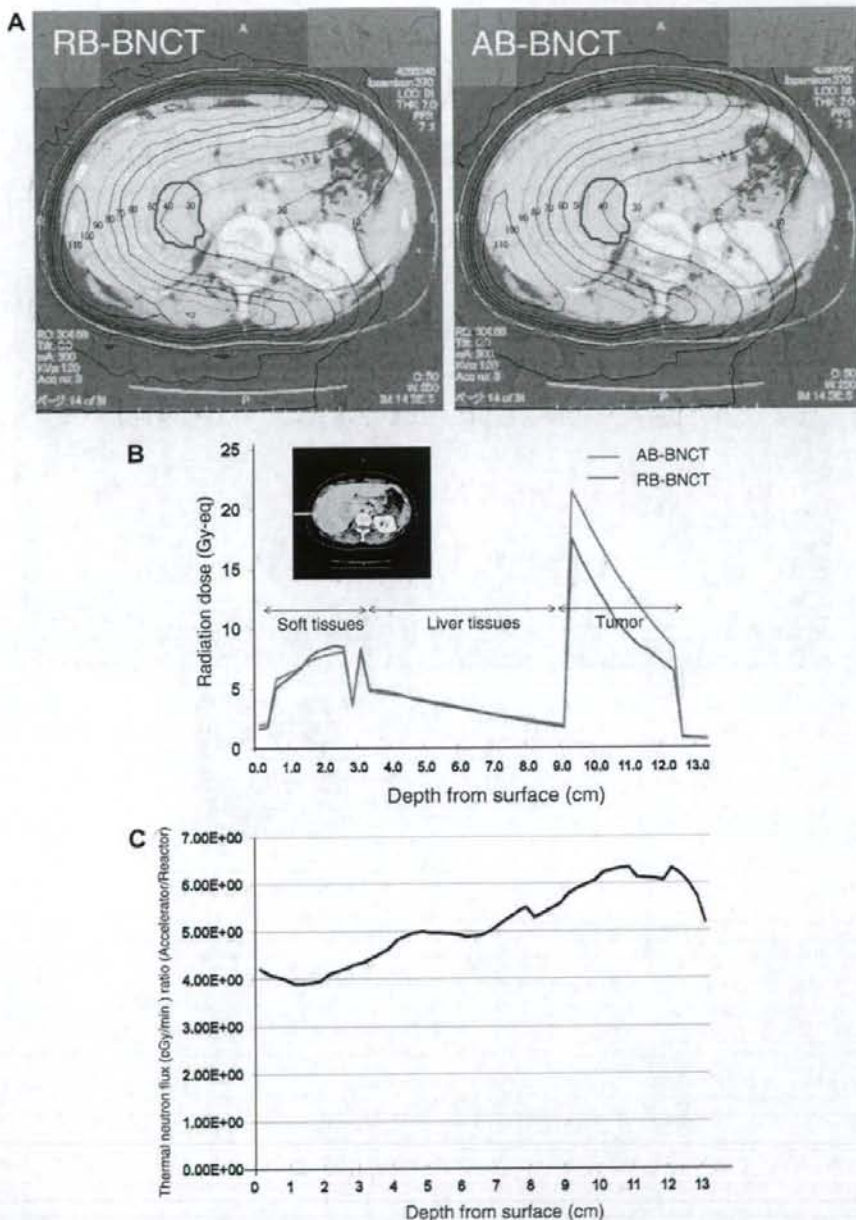


Fig. 3. (A) Comparison of isodose distribution between RB-BNCT and AB-BNCT. The liver tumor is contoured with a solid red line. (B) Depth-dose distribution profiles along the right neutron beam axis, which passed into the deep-seated liver tumor located at a depth of 9.5–12.5 cm. A yellow arrow on the CT image indicates the beam axis. (C) Depth-thermal neutron flux ratio (AB-BNCT to RB-BNCT) profiles along the same beam axis as that in (B).

299 BNCT, under conditions in which the mean doses delivered to normal
300 liver or lung are equal. This advantage of AB-BNCT over RB-
301 BNCT was especially evident in BNCT for deep-seated multiple liver
302 tumors. As shown in Table 2, AB-BNCT delivered significantly
303 greater doses to liver tumors than RB-BNCT did. As shown in
304 Fig. 2, the AB-BNCT system provided a higher peak energy (near
305 10 keV) in its neutron spectrum compared with RB-BNCT. The

higher energy peak of the AB-BNCT system is well suited for gener-
306 ating a thermal neutron flux distribution suitable for deep-
307 seated tumors and provides a larger thermal neutron fluence to
308 areas deep within the body compared to the RB-BNCT system.
309 However, while the epi-thermal neutron beam of HWNIF in the
310 KUR has a softer spectrum and the near-10-keV component is
311 not significant, the higher epi-thermal neutron component in-
312

Table 3

Irradiation time and DVH parameters showing averages (with range) for MPM tumors and normal lung.

Neutron source	Irradiation time (min)	Tumor			Ipsilateral lung			Contralateral lung			Liver ^a		
		D_{max} (Gy-eq)	D_{mean} (Gy-eq)	D_{min} (Gy-eq)	D_{max} (Gy-eq)	D_{mean} (Gy-eq)	D_{min} (Gy-eq)	D_{max} (Gy-eq)	D_{mean} (Gy-eq)	D_{min} (Gy-eq)	D_{max} (Gy-eq)	D_{mean} (Gy-eq)	D_{min} (Gy-eq)
KUR	134.7 (117.4–156.4)	40.0 (35.0–42.3)	19.9 (19.3–20.7)	4.3 (3.0–6.1)	7.7 (7.1–8.1)	5.0 ^b (7.1–8.1)	2.2 (1.8–2.5)	5.3 (4.7–6.8)	1.4 (1.2–1.9)	0.4 (0.3–0.6)	10.4 (10.0–10.8)	5.0 (4.6–5.2)	0.9 (0.8–1.0)
Accelerator	29.9 (26.3–33.3)	36.4 (33.0–38.3)	20.2 (19.7–21.0)	4.5 (3.4–6.4)	7.3 (6.9–7.5)	5.0 ^b (6.9–7.5)	2.3 (1.8–2.6)	4.9 (4.2–6.0)	1.3 (1.1–1.8)	0.3 (0.2–0.5)	9.7 (9.2–10.2)	5.0 (4.7–5.2)	0.8 (0.7–0.8)

Abbreviations: DVH = dose-volume histogram; MPM = malignant pleural mesothelioma; KUR = Kyoto University Research Reactor.

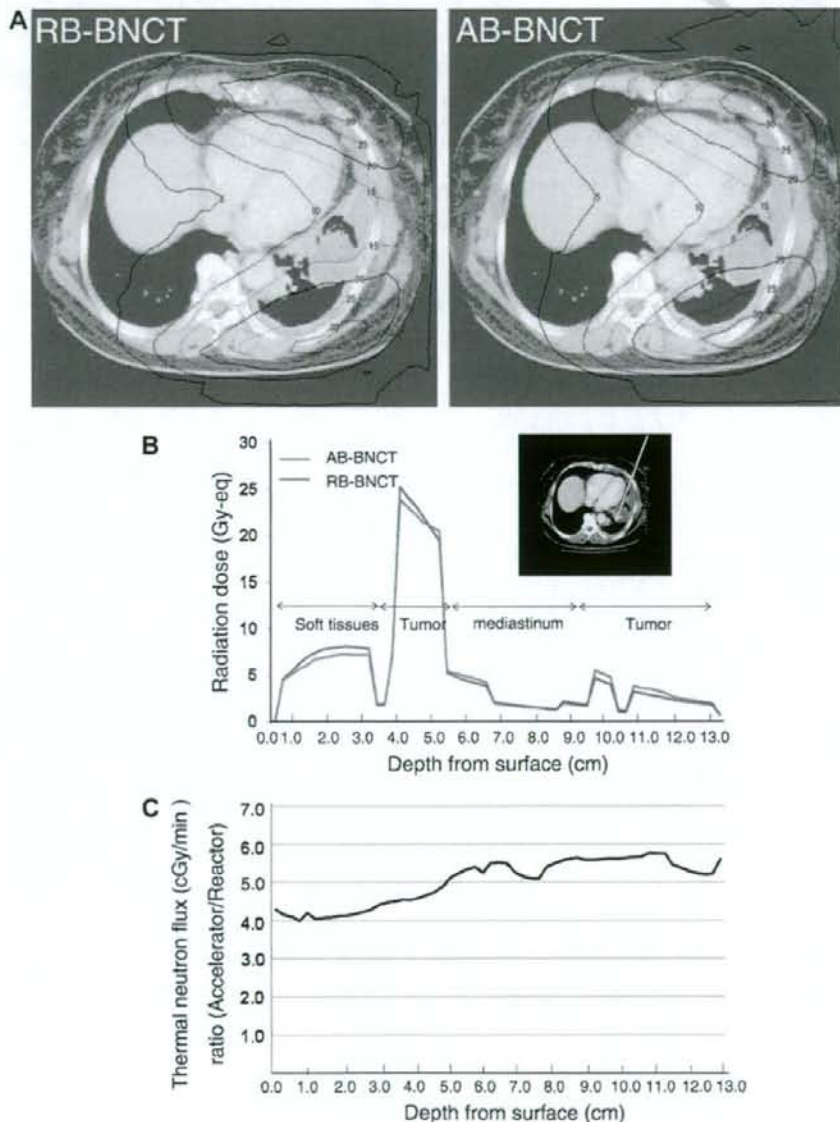
^a The average (range) of DVH data for liver was estimated using the data for three cases with right MPM.^b The mean dose to the liver normalized to 5.0 Gy-Eq.

Fig. 4. (A) Comparison of isodose distribution between RB-BNCT and AB-BNCT. (B) Depth-dose distribution profile along the anterior-oblique neutron beam axis in the case of BNCT for MPM. A yellow arrow on the CT image indicates the beam axis. (C) Depth-thermal neutron flux ratio (AB-BNCT to RB-BNCT) profiles along the same beam axis as that in (B).

cluded in the KUR beam is effective for enlarging the thermal neutron flux at parts deep within the body. This is because the RB-BNCT system can maximize the dose sent to deep-seated tumors near 10 cm, as well as the AB-BNCT system (Figs. 3B and 4B).

Some authors have already reported the advantage of AB-BNCT for deep-seated brain tumors over RB-BNCT using a head phantom. Burlon et al. have reported that AB-BNCT can treat brain tumors that are ~2.0 cm deeper than those treated with RB-BNCT [19]. Blue et al. have reported that, for treatment of brain tumors, compared with RB-BNCT, AB-BNCT can create a neutron field with a significantly better field quality (by a factor of 1.2), which is judged by the dose that can be delivered to a tumor at a depth of 6 cm [20]. The present study is believed to be the first to describe the advantages of AB-BNCT over RB-BNCT in the treatment of body trunk tumors, multiple liver tumors and MPM, apart from brain tumors.

We are preparing to undertake clinical trials with our AB-BNCT system to get an approval as a medical device from the Pharmaceuticals and Medical Devices Agency (PMDA), a Japanese regulatory agency. This approval is a prerequisite before the AB-BNCT system can be constructed at medical institutes. As revealed in the present study, AB-BNCT has the potential to be applied to multiple liver tumors and MPM. The patients with multiple liver tumors, including metastatic tumors or hepatocellular carcinomas, are much greater in number than malignant gliomas or melanomas, which have been treated with BNCT in Japan, the United States and Europe. Selective high-LET irradiation to tumor cells by BNCT has the potential to shed new light on the best way to treat multiple metastatic tumors in lung or brain and pleuritis carcinomatosis. Extending the application of BNCT to many malignancies will lead to further progress in the field of BNCT. After approval of the AB-BNCT system as a medical device, it will be on the market and installed in existing hospitals.

In conclusion, the AB-BNCT system under construction at our institute has the ability to deliver three- or four-port irradiation in the treatment of multiple liver tumors and MPM within a reasonable treatment time (30–60 min). In addition, the AB-BNCT system has advantages over RB-BNCT for the treatment of deep-seated tumors. AB-BNCT has the potential to be a promising treatment option for patients with multiple liver tumors and MPM.

References

[1] Coderre JA, Morris GM. The radiation biology of boron neutron capture therapy. *Radiat Res* 1999;151:1–18.

[2] Barth RF, Joensuu H. Boron neutron capture therapy for the treatment of glioblastomas and extracranial tumours: as effective, more effective or less effective than photon irradiation? *Radiother Oncol* 2007;82:119–22.

[3] Suzuki M, Masunaga S, Kinashi Y, et al. Intra-arterial administration of sodium borocaptate (BSH)/lipiodol emulsion delivers B-10 to liver tumors highly selectively for boron neutron capture therapy: experimental studies in the rat liver model. *Int J Radiat Oncol Biol Phys* 2004;59:260–6.

[4] Suzuki M, Sakurai Y, Masunaga S, et al. Preliminary experimental study of boron neutron capture therapy for malignant tumors spreading in thoracic cavity. *Jpn J Clin Oncol* 2007;37:245–9.

[5] Suzuki M, Sakurai Y, Masunaga S, Kinashi Y, Nagata K, Ono K. Dosimetric study of boron neutron capture therapy with borocaptate sodium (BSH)/lipiodol emulsion (BSH/lipiodol-BNCT) for treatment of multiple liver tumors. *Int J Radiat Oncol Biol Phys* 2004;58:892–6.

[6] Suzuki M, Sakurai Y, Masunaga S, et al. Feasibility of boron neutron capture therapy (BNCT) for malignant pleural mesothelioma from a viewpoint of dose distribution analysis. *Int J Radiat Oncol Biol Phys* 2006;66:1584–9.

[7] Suzuki M, Sakurai Y, Hagiwara S, et al. First attempt of boron neutron capture therapy (BNCT) for hepatocellular carcinoma. *Jpn J Clin Oncol* 2007;37:376–81.

[8] Suzuki M, Endo K, Satoh H, et al. A novel concept of treatment of diffuse or multiple pleural tumors by boron neutron capture therapy (BNCT). *Radiother Oncol* 2008;88:192–5.

[9] Lee CL, Zhou XL, Kudchadker RJ, Harmon F, Harker YD. A Monte Carlo dosimetry-based evaluation of the $^7\text{Li}(p,n)^7\text{Be}$ reaction near threshold for accelerator boron neutron capture therapy. *Med Phys* 2000;27:192–202.

[10] Tanaka H, Sakurai Y, Suzuki M, et al. An epithermal neutron generator based on the $\text{Be}(p,n)$ reaction using a 30 MeV proton cyclotron accelerator at KURRI. In: Zonta A, Altieri S, Roveda L, Barth R, editors. 13th International Congress on Neutron Capture Therapy "A new option against cancer". Roma: ENEA; 2008. p. 510–3.

[11] IAEA. Current status of neutron capture therapy. In: IAEA TECDOC 1223. Vienna: IAEA; 2001. p. 6–8.

[12] Sakurai Y, Kobayashi T. Controllability of depth dose distribution for neutron capture therapy at the heavy water neutron irradiation facility of Kyoto University Research Reactor. *Med Phys* 2002;29:2338–50.

[13] Sakurai Y, Kobayashi T. The medical-irradiation characteristics for neutron capture therapy at the heavy water neutron irradiation facility of Kyoto University Research Reactor. *Med Phys* 2002;29:2328–37.

[14] Kawabata S, Miyatake S, Kajimoto Y, et al. The early successful treatment of glioblastoma patients with modified boron neutron capture therapy. Report of two cases. *J Neurooncol* 2003;65:159–65.

[15] Kato I, Ono K, Sakurai Y, et al. Effectiveness of BNCT for recurrent head and neck malignancies. *Appl Radiat Isot* 2004;61:1069–73.

[16] Suzuki M, Masunaga S, Kinashi Y, et al. The effects of boron neutron capture therapy on liver tumors and normal hepatocytes in mice. *Jpn J Cancer Res* 2000;91:1058–64.

[17] Kiger JL, Kiger WS, Patel H, et al. Functional and histological assessment of the radiobiology of normal rat lung in BNCT. In: Nakagawa Y, Kobayashi T, Fukuda H, editors. Advances in neutron capture therapy 2006. Takamatsu: ISNCT; 2006. p. 85–8.

[18] Ono K, Nagata Y, Akuta K, Abe M, Ando K, Koike S. Frequency of micronuclei in hepatocytes following X and fast-neutron irradiations—an analysis by a linear-quadratic model. *Radiat Res* 1990;123:345–7.

[19] Burlon AA, Kreiner AJ. A comparison between a TESQ accelerator and a reactor as a neutron sources for BNCT. *Nucl Instr Meth Phys Res B* 2008;266:763–71.

[20] Blue TE, Yanch J. Accelerator-based epithermal neutron sources for boron neutron capture therapy of brain tumors. *J Neurooncol* 2003;62:19–31.